

# Hole-Burning and Absorption Studies of the LH1 Antenna Complex of Purple Bacteria: Effects of Pressure and Temperature

H.-M. Wu,<sup>†</sup> M. Rätsep,<sup>†</sup> R. Jankowiak,<sup>†</sup> R. J. Cogdell,<sup>‡</sup> and G. J. Small<sup>\*,†</sup>

Ames Laboratory-USDOE and Department of Chemistry, Iowa State University, Ames, Iowa 50011, and Division of Biochemistry and Molecular Biology, Institute of Biomedical and Life Sciences, University of Glasgow, G12 8QQ, U.K.

Received: December 4, 1997; In Final Form: March 5, 1998

Spectral hole-burning and absorption spectroscopies were combined with pressure and temperature in studies of the light harvesting 1 (LH1 or B875) antenna complex of wild-type (WT) chromatophores and an LH1-only mutant of *Rhodobacter sphaeroides*. Zero-phonon hole (ZPH) action spectra lead to values of 120 (WT) and 140 cm<sup>-1</sup> (mutant) for the separation ( $\Delta E$ ) between the lowest energy exciton level of A symmetry, B896, and the adjacent, strongly absorbing E<sub>1</sub> level of the C<sub>16</sub> ring of 32 bacteriochlorophyll *a* molecules. The E<sub>1</sub> level is responsible for most of the B875 band's absorption intensity. Values for the inhomogeneous broadening of the relatively weak B896 absorption band are given. High-pressure hole-burning data for the B896 band yielded a very large linear pressure shifting of -0.67 cm<sup>-1</sup>/MPa, about 10% higher than the shift rate for the B875 absorption band. These shifts are about a factor of 7 times higher than those of weakly coupled chlorophyll molecules in protein complexes and isolated chromophores in polymers and glasses. A theoretical model is presented which leads to the conclusion that electron-exchange coupling between nearest neighbor BChl *a* molecules of the B875 ring is largely responsible for the large pressure shifts. (Such coupling produces charge-transfer (CT) states which mix with the neutral <sup>1</sup> $\pi\pi^*$  states of the BChl *a* molecules.) It follows that a firm understanding of the excitonic structure of the B875 ring is unachievable by consideration of only electrostatic interactions. These conclusions also apply to the B850 BChl *a* ring of the LH2 complex. The data from the pressure studies can be used as benchmarks for electronic structure calculations which take into account both electrostatic and CT interactions. Thermal broadening and shifting data for the B875 band establish that the LH1 complex undergoes a nondenaturing structural change at ~150 K in a glycerol/water glass, as has been reported for the LH2 complex. The structural change occurs for chromatophores and isolated complexes. The ability to detect the subtle structural change via the B875 and B850 bands is a consequence of strong coupling between BChl *a* molecules of the B875 and B850 rings. The results of the high-pressure experiments indicate that CT is an important contributor to the coupling and that the structural change may not be detectable by X-ray diffraction at typical ~2 Å resolution. Theoretical models from Wu et al. (*J. Phys. Chem. B* 1997, 101, 7641) provide a satisfactory explanation for the thermal shifting and broadening of the B875 band. The broadening is dynamic, the result of interexciton level downward relaxation triggered by a low-frequency, intermolecular promoting mode(s) which modulate nearest neighbor couplings. The nearest neighbor BChl *a*-BChl *a* couplings for the low-temperature structure of the B875 ring are estimated to be 30% stronger than those of the high-temperature structure.

## 1. Introduction

The bacteriochlorophyll (BChl) antenna network of purple bacteria such as *Rhodobacter sphaeroides*, *Rhodospirillum rubrum*, and *Rhodopseudomonas acidophila* is composed of a light harvesting 2 (LH2) and LH1 protein complex which act in concert to funnel solar energy to the reaction center (RC) complex. The LH2 and LH1 complexes of the first two species and strain 10050 of *Rps. acidophila* are often referred to as B800-850 and B875, respectively, because of the approximate locations, in nm, of their BChl *a* Q<sub>y</sub>(S<sub>1</sub>) absorption bands at room temperature. The basic B800 → B850, B850 → B875, and B875 → RC excitation energy transfer processes, which occur on a picosecond time scale, and the Q<sub>y</sub> states of the interacting BChl *a* molecules held in place by protein scaffolding

have long been subjects of very considerable interest (for reviews see refs 1-3).

Recently, the X-ray structure of the LH2 complex of *Rps. acidophila* (strain 10050) was reported at a resolution of 2.5 Å.<sup>4</sup> The structure revealed that this complex is a cyclic 9-mer of  $\alpha/\beta$  polypeptide pairs. The arrangement of the BChl *a* molecules is shown in Figure 1, where the arrows, which lie nearly in the membrane plane, indicate the direction of Q<sub>y</sub> transition dipoles. Several Mg...Mg separation distances are indicated. The relatively large separation of 21 Å between adjacent B800 molecules results in weak coupling,  $V \sim -20$  cm<sup>-1</sup>,<sup>5</sup> consistent with hole burning data that indicated that excitonic effects are unimportant for the B800 ring.<sup>6-8</sup> However, the B850 nearest neighbor distances of 8.9 and 9.6 Å lead to large coupling energies,  $V \sim +300$  cm<sup>-1</sup>.<sup>5,9</sup> Figure 1 shows that the B850 ring of 18 BChl *a* molecules should be viewed as a 9-mer of dimers. There are, however, two choices for the

<sup>†</sup> Iowa State University.

<sup>‡</sup> University of Glasgow.

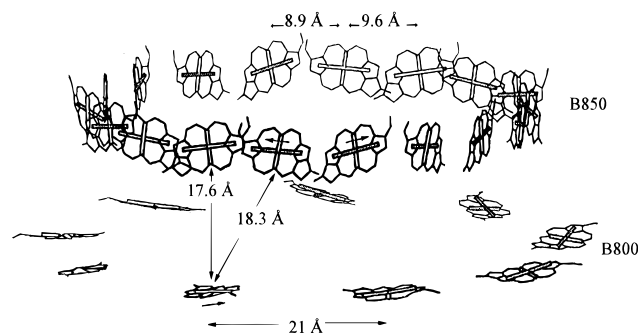


**Figure 1.** Schematic (based on Figure 1 in ref 5) showing the arrangement of the 18 B850 (upper ring) and 9 B800 (lower ring) BChl *a* molecules in the LH2 antenna complex from *Rps. acidophila*. Within the circular array, nearest neighbor distances (Mg...Mg) between B850 molecules are either 8.9 or 9.6 Å. The 9.6 Å distance is that of the two BChl *a* molecules associated with the  $\alpha,\beta$  polypeptide pair. The two B850 BChl *a* molecules nearest to a B800 molecule are separated by distances of 17.6 and 18.3 Å. The horizontal arrows indicate the directions of the  $Q_y$  transition dipoles.

dimer, one associated with the 8.9 Å separation distance and the other with the distance of 9.6 Å. From an excitonic structure point of view, however, the choice of dimer is inconsequential. The monomers of either dimer are symmetry-inequivalent, and so, strictly speaking, the dimers should be referred to as heterodimers. More recently, the X-ray structure of the isolated LH2 or B800–850 complex of *Rhodospirillum rubrum* was reported.<sup>10</sup> Interestingly, LH2 was shown to be an 8-mer of  $\alpha,\beta$  polypeptide pairs. A comparison of the two structures is given by Koepke et al.<sup>10</sup> Suffice it to say that the picture that has the B800 molecules weakly coupled and the B850 molecules strongly coupled remains intact for LH2 of *Rs. rubrum* and orientations of the B850 molecules relative to each other very similar to those of *Rs. rubrum*. An X-ray structure of the LH2 complex from *Rb. sphaeroides* has yet to be determined. Concerning the LH1 complex of *Rs. rubrum*, it is a cyclic 16-mer of BChl *a* dimers with an inner core large enough to house the RC complex.<sup>11</sup> Unfortunately, the resolution of the electron micrographs is too low to permit electronic structure calculations of the type reported for the LH2 complex of *Rps. acidophila*.<sup>5,9</sup> However, the energy minimization and molecular dynamics simulations of Hu et al.<sup>12</sup> indicate that the structural arrangement of LH1's BChl *a* molecules is similar to that shown in Figure 1, the main difference being the larger ring size of LH1.<sup>13</sup>

These striking cyclic nanostructures have stimulated further femtosecond pump–probe<sup>14–20</sup> and spectral hole burning studies of the electronic structure and excitation energy transfer processes of the LH2 and LH1 complexes. As a result, for example, the weak dependence of the B800  $\rightarrow$  B850 1–2 ps kinetics on temperature, pressure, species, and mutation which, in combination, lead to a variation in the B800–B850 energy gap from  $\sim 450$  to  $1050\text{ cm}^{-1}$ , can be understood in terms of weak coupling Förster theory with spectral overlap provided by BChl *a* vibronic and protein phonon transitions<sup>8,21</sup> (see ref 2 for further discussion). This mechanism was originally proposed by Reddy et al.<sup>22</sup> on the basis of hole burning data. The theoretical calculations in ref 8 took into account the inhomogeneous and homogeneous broadenings of the B800 and B850 absorption bands and, insofar as the resilience of B800  $\rightarrow$  B850 transfer against significant variations in the electronic energy gap is concerned, involved no adjustable parameters. Very recently, Fowler et al.<sup>23</sup> reported results on the B800  $\rightarrow$  B850 transfer kinetics in a series of *Rb. sphaeroides* mutants

designed to alter the position of the B800 band. The variation in the transfer rate with changing B800–B850 energy gap was satisfactorily explained using the theoretical model of refs 16 and 24. During the course of time domain and hole-burning studies<sup>16,25–27</sup> of the B800  $\rightarrow$  B850 energy-transfer process, it was observed that excitation on the high-energy side of the B800 absorption band results in downward subpicosecond relaxation ( $\sim 0.4\text{ ps}$ ) within the B800 band. Several possible mechanisms for this relaxation were considered in ref 16, one of which involves coupling of B800 molecules with quasi-degenerate upper exciton levels of the B850 ring. However, additional studies are required before this intra-B800 band relaxation can be said to be understood.

Femtosecond pump–probe experiments yielded results that indicate that downward relaxation between the exciton levels that contribute to the B850 and B875 bands occurs on a 100 fs time scale,<sup>17,28,29</sup> consistent with earlier hole burning data.<sup>7,30</sup>

Calculations of the  $Q_y$  electronic structure of the LH2 complex of *Rps. acidophila* based on the room-temperature X-ray structure have also been performed.<sup>5,9</sup> In ref 5 only electrostatic interactions were considered, while in ref 9 charge-transfer (CT) interactions were also taken into account. The results of both works led to the conclusion that the B800 molecules have only a weak effect on the excitonic level structure of the strongly coupled BChl *a* molecules of the B850 ring (see Figure 2 of this paper for an exciton level structure of this ring calculated in the absence of B800–B850 BChl *a* interactions). It is important to note that testing of the results of the electronic structure calculations often involves low-temperature spectroscopic data.

With this in mind, the recent finding that<sup>31,32</sup> the LH2 complexes of the three aforementioned species, whether the complex is isolated or in chromatophores, undergo a non-denaturing structural change near  $150\text{ K}$ <sup>31,32</sup> is important. This finding was based on the temperature dependence ( $4.2\text{--}250\text{ K}$ ) of the LH2  $Q_y$  absorption spectrum. The theoretical model presented in ref 32 led to the conclusion that the nearest neighbor BChl *a*–BChl *a* couplings of the B850 ring are considerably stronger for the low-temperature structure. The assumptions of the model are further examined in this paper since we present results on the temperature dependence of the B875 absorption band.

Another recent development is that static energy disorder (diagonal and/or off-diagonal) from the glasslike structural heterogeneity of proteins is important for understanding the exciton level structure of the B850 and B875 rings<sup>9,12,15,31,33–35</sup> of BChl *a* molecules. This disorder is intimately connected with the significant inhomogeneous broadening ( $\Gamma_{\text{inh}}$ ) of the B850 and B875 absorption bands as well as the B800 band.<sup>7,16,22,25,36</sup> Such broadening for photosynthetic complexes at low temperatures has been characterized by hole-burning spectroscopy.<sup>37–39</sup> For high-quality samples  $\Gamma_{\text{inh}} \sim 50\text{--}150\text{ cm}^{-1}$ , depending on the complex. It has recently been argued that  $\Gamma_{\text{inh}}$  at room temperature can be just as large.<sup>29,40–42</sup> Energy disorder destroys the  $C_n$  symmetry, splits degeneracies of exciton levels, and mixes different zero-order levels, causing a redistribution of oscillator strength.<sup>9,33,43</sup> Quite detailed studies of these effects from energy disorder on the exciton levels associated with the B850 band have been reported<sup>33,35,43</sup> in which symmetry-adapted basis energy defect patterns (BDP) were used for systematic analysis. Experimental data were used to argue that for the B850 ring one is in the weak disorder regime, meaning that the disorder-induced coupling matrix elements between energetically different exciton levels are comparable to or smaller than the

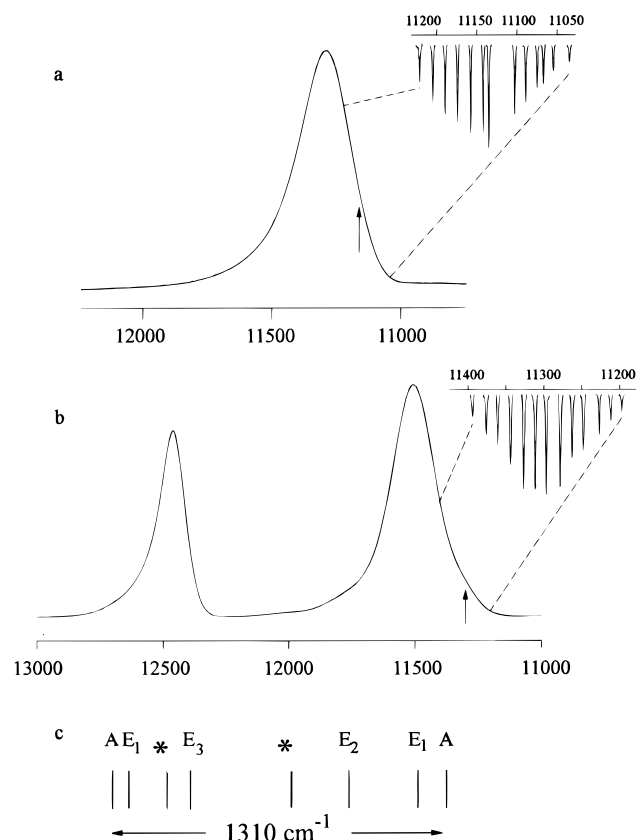


**Figure 2.** (a) 4.2 K B875 absorption and B896's zero-phonon hole (ZPH) action spectrum (read resolution =  $0.8\text{ cm}^{-1}$ ) for the LH1-only mutant of *Rb. sphaeroides*. (b) 4.2 K B850 absorption and B870's zero-phonon hole (ZPH) action spectrum (read resolution =  $0.5\text{ cm}^{-1}$ ) for LH2 of *Rps. acidophila*. The ZPH action spectra in a and b were generated with a constant burn fluence of 50 and  $100\text{ J/cm}^2$ , respectively. The arrows locate the center of the action spectra ( $140$  and  $200\text{ cm}^{-1}$  below the B875 and B850 band maximum, respectively). The fractional OD changes for ZPH at the arrows are 0.11 and 0.15 for B896 and B870, respectively. The action spectrum carries an inhomogeneous width of  $150 \pm 10\text{ cm}^{-1}$  in a and  $120 \pm 10\text{ cm}^{-1}$  in b. Also shown together is the calculated exciton manifold of the B850 ring (c) from Figure 2 of ref 34. The strongly absorbing  $E_1$  level in the lower manifold is placed at B850 absorption maximum. The asterisks indicate two closely spaced doubly degenerate levels. For easy comparison, the absorption spectra and the exciton levels are shown in the same wavenumber scale, while the  $x$ -axis of the action spectra has been expanded 3-fold.

zero-order level spacings. Static disorder leads to localization effects, meaning that the exciton level wave functions are no longer perfectly delocalized (extended). Such localization is not dynamic since it emerges from Schrödinger's time-independent equation. An example of dynamic localization is self-trapping at a site on the ring due to the exciton-phonon interaction (for a recent discussion see ref 44). Currently, localization-extendedness (LE) associated with the B850 and B875 ring exciton levels and its effect on superradiance and two-exciton absorption transitions are attracting considerable attention.<sup>19,42,44–46</sup>

From recent works on the LH2 and LH1 complexes, many of which are referenced above, it is apparent that a firm understanding of their excitation energy transfer/relaxation dynamics requires accurate zero-order (no energy disorder) excitonic Hamiltonians as well as Hamiltonians that accurately describe the effects of energy disorder. The attainment of such requires high-resolution experimental data that, for example, determine whether the energy disorder is weak or strong. Our approach is one that involves hole-burning and absorption

spectroscopies combined with pressure and temperature and theoretical modeling.<sup>32,33,35,43</sup> This approach is followed here where we present new results on the B875 band of the LH1 complex, including data that locate and characterize the lowest energy exciton level (A symmetry), often referred to as B896. (The corresponding level of the B850 ring is referred to as B870.) Comparisons of the pressure and temperature dependencies of the B875 band of *Rb. sphaeroides* with those of the B850 band of *Rb. sphaeroides*<sup>32</sup> and *Rps. acidophila*,<sup>31,32</sup> as well as a comparison of the linear pressure shifting and broadening of the B896 and B870 zero-phonon holes, are given.

The main questions addressed in this paper are as follows: does the LH1 complex also undergo a nondenaturing structural change near 150 K; are electron-exchange interactions or, equivalently, is the mixing of charge-transfer (CT) states with the  $Q_y(\pi\pi^*)$  states of the B850 and B875 rings important for understanding their excitonic structures; and are the nearest neighbor BChl  $a$ –BChl  $a$  couplings of the B875 rings stronger than those of the B850 ring.

## 2. Experimental Section

The LH2 complexes of *Rps. acidophila* (strain 10050) and *Rb. sphaeroides* were isolated according to the procedure described in ref 47. After dilution in glycerol/water solution (2:1 by volume) containing 0.1% LDAO in water, samples were contained in a polypropylene cryogenic tube and cooled in a Janis 8-DT liquid helium cryostat. Typical values for the optical density at the B850 band maximum were close to 0.5. The conditions used for chromatophores of these two species were the same as for the isolated complexes. The LH1-only mutant ( $\Delta$ RC-1A) was kindly provided by Dr. Joanne Williams of Arizona State University. The mutant was grown semiaerobically in the presence of tetracyclin, in a shaking incubator at  $30\text{ }^\circ\text{C}$  with succinate as the carbon source. The level of aeration was controlled so that the synthesis of LH1 still occurred even though the cells were growing by respiration. After growth the cells were harvested by centrifugation and broken by sonication and the photosynthetic membranes were collected by centrifugation. The membranes were resuspended in 20 mM Tris HCL pH 8.0. Due to a higher lipid-to-protein ratio than in normal chromatophores, 3% of  $\beta$ -octylglucoside in water/glycerol mixture (1:2 by volume) was used to solubilize the LH1-only membrane. A Bruker IFS 120HR Fourier transform spectrometer was used to record the preburn and postburn spectra. The burn laser was a Coherent CR 899-21 Ti:sapphire laser (line width of  $0.07\text{ cm}^{-1}$ ) pumped by a 15 W Coherent Innova 200 Ar-ion laser. Burn fluences, burn wavelengths, and read resolutions are given in the figure captions. A detailed description of the hole-burning apparatus can be found in ref 48. For temperature dependence studies, a Lake Shore temperature controller (model 330) was used to stabilize the temperature. After the diode reading reached the preset temperature, the sample was allowed to equilibrate for 15 min prior to initiating absorption or hole burning measurements.

The high-pressure apparatus has been described in detail,<sup>49</sup> including the procedure used to measure pressure. To ensure good optical quality, the sample was contained in a gelatin capsule (5 mm outside diameter) and then housed in a specially designed high-pressure cell (maximum pressure rating of 800 MPa) with four sapphire windows (thickness of 4 mm) providing optical access. The cell was connected to a three-stage hydraulic compressor (model U11, Unipress Equipment Division, Polish Academy of Sciences) through a flexible thick-walled capillary (o.d./i.d. = 3.0 mm/0.3 mm). Helium gas was used as the

TABLE 1: Absorption Band Properties at 4.2 K<sup>a</sup>

|                                  | Wild-Type Chromatophores                   |                         |                        |        |
|----------------------------------|--------------------------------------------|-------------------------|------------------------|--------|
|                                  | <i>Rps. acidophila</i>                     |                         | <i>Rb. sphaeroides</i> |        |
|                                  | B850                                       | B875                    | B850                   | B875   |
| $\nu_{\max}$ (cm <sup>-1</sup> ) | 11 490                                     | 11 045                  | 11 715                 | 11 220 |
| $\Gamma$ (cm <sup>-1</sup> )     | 215                                        | 195                     | 230                    | 195    |
| $\Delta E$ (cm <sup>-1</sup> )   |                                            |                         |                        | 120    |
|                                  | Isolated LH2 Complexes and LH1-Only Mutant |                         |                        |        |
|                                  | <i>Rps. acidophila</i>                     |                         | <i>Rb. sphaeroides</i> |        |
|                                  | B850 (LH2) <sup>b</sup>                    | B850 (LH2) <sup>c</sup> | B875 (LH1)             |        |
| $\nu_{\max}$ (cm <sup>-1</sup> ) | 11 500                                     | 11 730                  | 11 290                 |        |
| $\Gamma$ (cm <sup>-1</sup> )     | 200                                        | 245                     | 245                    |        |
| $\Delta E$ (cm <sup>-1</sup> )   | 200                                        | 185                     | 140                    |        |

<sup>a</sup> The widths of the B800 band for *Rps. acidophila* and *Rb. sphaeroides* are 125 cm<sup>-1</sup>. <sup>b</sup> Refs 32, 34. <sup>c</sup> Ref 32.

pressure-transmitting medium. With compression ratios of about 1, 5, and 79 for the three stages of the compressor, the highest hydrostatic pressure achievable is 1.5 GPa. A specially designed Janis 11-DT cryostat was used for cooling of the high-pressure cell. High-pressure hole-burning was performed at 12 K. At this temperature liquid helium solidifies at ~75 MPa. Following the procedure of refs 49–51, it was confirmed that pressure-induced structural changes are elastic.

### 3. Results

**Zero-Phonon Action Spectrum for B896 of the LH1 Complex.** The lower absorption spectrum of Figure 2 is that of the isolated LH2 complex of *Rps. acidophila* at 4.2 K from ref 32. The bands near 11 500 and 12 500 cm<sup>-1</sup> are B850 and B800, respectively, with widths (fwhm) of 200 and 125 cm<sup>-1</sup>; see Table 1. The absorption profile shapes for *Rb. sphaeroides* are very similar<sup>32</sup> as are their widths, Table 1. However, the B800–B850 energy gap for *Rb. sphaeroides* is significantly smaller than that of *Rps. acidophila* (also *Rs. molischianum*) at all temperatures, by ~200 cm<sup>-1</sup> at 4.2 K,<sup>32</sup> Table 1. The diminution in this energy gap is mainly due to the B850 band of *Rps. acidophila* being red-shifted relative to that of *Rb. sphaeroides*.<sup>32</sup> At the bottom of Figure 2 is the exciton energy level diagram for the B850 ring for *Rps. acidophila* from ref 34 calculated in the nearest dimer–dimer coupling approximation.<sup>52</sup> In the absence of energy disorder, the E<sub>2</sub>, E<sub>3</sub>, and E<sub>4</sub> levels are symmetry forbidden in absorption from the ground state. However, the structure of the complex that leads, in part, to the Q<sub>y</sub> transition dipoles lying nearly in the membrane plane (perpendicular to the C<sub>9</sub> axis) results in the lowest energy E<sub>1</sub> level carrying almost all of the absorption intensity. For example, the lowest energy A level (B870) is predicted to carry less than 1% of the B850 band intensity.<sup>5,9</sup> Thus, in Figure 2 the lowest E<sub>1</sub> level is placed at the B850 band maximum. Set off to the upper right is the B870 ZPH action spectrum<sup>53</sup> whose overall profile faithfully represents the B870 absorption profile with  $\Gamma_{\text{inh}} = 120 \pm 10$  cm<sup>-1</sup> and band maximum indicated at the position of the upward solid arrow. The displacement of the A level (B870) below the B850 maximum (or E<sub>1</sub> level) is defined as  $\Delta E$  and equals 200 cm<sup>-1</sup>, Table 1. The weak shoulder on the low-energy side of the B850 band is due to B870, which carries 3–5% of the intensity of the entire B850 band.<sup>32,34</sup> It proved necessary to invoke energy disorder and to consider the structural change near 150 K (see section 1) in order to account for this intensity and that  $\Delta E = 200$  cm<sup>-1</sup> is ~100 cm<sup>-1</sup> larger than the calculated room-temperature value.<sup>32,34</sup> The 4.2 K absorption profile of B875 for the LH1-only mutant

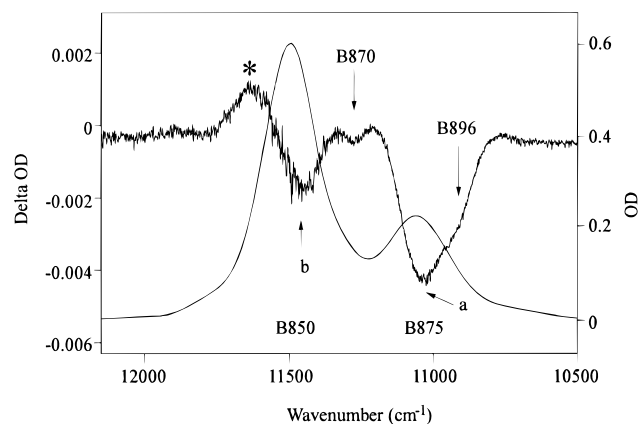


**Figure 3.** 4.2 K absorption and non-line-narrowed hole-burned spectra of *Rps. acidophila* chromatophores. The B850 and B875 band maxima (widths) are 11 495 (220) cm<sup>-1</sup> and 11 060 (255) cm<sup>-1</sup>. The burn frequency of 12 473 cm<sup>-1</sup> located in the B800 band produced a 7% deep ZPH (not shown). The burn fluence employed was 225 J/cm<sup>2</sup>. See text for other details.

is shown at the top of Figure 2 along with ZPH action spectrum of B896, for which  $\Gamma_{\text{inh}} = 150 \pm 10$  cm<sup>-1</sup> and  $\Delta E = 140 \pm 10$  cm<sup>-1</sup>. For wild-type chromatophores of *Rb. sphaeroides*  $\Delta E = 120 \pm 10$  cm<sup>-1</sup> (B896 ZPH action spectrum not shown). Table 1 summarizes the above results and includes those for the B850 band of *Rb. sphaeroides* from ref 32.

It is instructive to show the hole-burned spectrum of *Rb. sphaeroides* chromatophores obtained under non-line-narrowing conditions (laser excitation into the B800 band). Following energy transfer to the B850 and B875 molecules (levels), nonphotochemical hole burning occurs to produce broad hole features in the B850 and B875 bands, Figure 3. The features labeled as a and b are holes associated with the main part (E<sub>1</sub> levels) of the B875 and B850 bands. Feature \* is the antihole of hole b. Clearly evident are the B870 and B896 holes. Their displacements from holes b and a are  $\Delta E \approx 170$  and 120 cm<sup>-1</sup>, respectively, in reasonable agreement with the values obtained by ZPH action spectroscopy, Table 1.

#### Temperature Dependence of the B875 Absorption Band.

The dependencies of the B875 absorption bandwidth (fwhm) and peak position (solid circles) on temperature are shown in Figure 4. That the B875 band does not shift until ~150 K is what has been reported for the B850 bands of *Rps. acidophila*, *Rb. sphaeroides*, and *Rs. molischianum* (isolated LH2 and chromatophores).<sup>31,32</sup> The linear shifting to the blue at temperatures higher than ~150 K is also observed for the B850 band. Linear shift rates are given in Table 2. The temperature of 150 K is close to the glass transition temperature ( $T_g$ ) of the glycerol/water glass-forming solvent. The significant reduction in viscosity above  $T_g$  allows for structural changes of the protein complex as discussed in refs 54 and 55. With this in mind, it is important to note that the position of the B800 band is invariant to temperature from 4 to 300 K ( $\pm 5$  cm<sup>-1</sup> uncertainty),<sup>31,32</sup> suggesting that the strong BChl *a*–BChl *a* couplings of the B850 and B875 rings are primarily responsible for the linear shifting above 150 K. The invariance of the B800, B850, and B875 band positions below 150 K means that the LH1 and LH2 structures change little below this temperature.<sup>31,32</sup> Turning next to the thermal broadening data for the B875 band in Figure 4, one sees that above about 150 K the broadening varies linearly with temperature with a rate of 0.84 cm<sup>-1</sup>/K. The solid curve below 150 K is a theoretical fit; see section 4. Between ~50 and ~150 K, however, the broadening is also linear with temperature, 1.08 cm<sup>-1</sup>/K. The distinct break in the linear

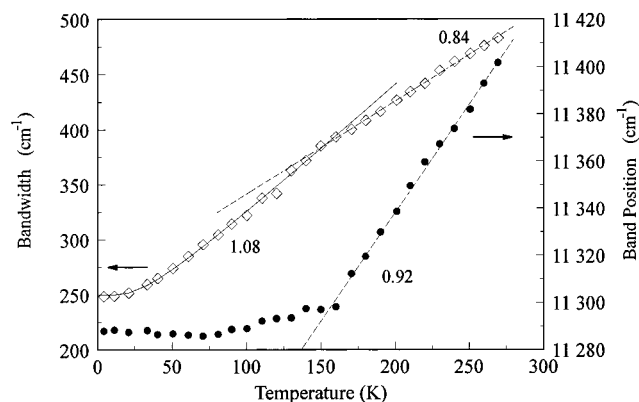


**Figure 4.** Temperature dependencies of the B875 band position (solid circles) and bandwidth (diamonds) for the LH1-only mutant of *Rb. sphaeroides*. Linear regression lines (dashed lines), together with their slopes (in units of  $\text{cm}^{-1} \text{K}^{-1}$ ), for the bandwidths (fwhm) and the band maxima are shown in the region above  $\sim 150 \text{ K}$  to emphasize the linear dependence. The band maximum remains constant ( $\pm 5 \text{ cm}^{-1}$ ) in the low-temperature region. The solid curve is the fit for B875 bandwidths using eq 12; see text for details. Above  $\sim 50 \text{ K}$ , the bandwidths and the fit curve become linear, which can be described by a regression line (not shown) with a slope of  $1.08 \text{ cm}^{-1} \text{K}^{-1}$ . See Table 3 for the uncertainties of the slopes.

**TABLE 2: Temperature-Dependent Data for Isolated LH2 from *Rps. acidophila* and *Rb. sphaeroides*, and LH1-Only Mutant of *Rb. sphaeroides*<sup>a</sup>**

|                                     |        | <i>Rb. sphaeroides</i>  |                    |                 |
|-------------------------------------|--------|-------------------------|--------------------|-----------------|
|                                     |        | <i>Rps. acidophila</i>  | B850               | B875            |
|                                     |        | B850 (LH2) <sup>b</sup> | (LH2) <sup>c</sup> | (LH1)           |
| (cm <sup>-1</sup> K <sup>-1</sup> ) |        |                         |                    |                 |
| shift rate                          |        | $0.87 \pm 0.03$         | 0.39               | $0.92 \pm 0.02$ |
| broadening rate                     | low T  | 0.64                    | 0.52               | $1.08 \pm 0.04$ |
|                                     | high T | 0.47                    | 0.36               | 0.84            |

<sup>a</sup> The uncertainties for the rates are  $\pm 0.01 \text{ cm}^{-1} \text{K}^{-1}$  except for those indicated in the table. <sup>b</sup> Ref 32. <sup>c</sup> Ref 32.

broadening at 150 K should be noted. This behavior is also observed for the B850 bands of *Rps. acidophila* and *Rb. sphaeroides*;<sup>31,32</sup> see Table 2 for comparison of linear broadening rates. In refs 31 and 32 the linear broadening was interpreted in terms of downward interexciton level relaxation by one-phonon emission; see section 4. Apparently, the break in the linear broadening at 150 K is connected with the non-denaturing structural change of the complexes near 150 K. The thermal broadening seen in Figure 4 for B875 is very different from that for the B800 band (recall that the B800 molecules are weakly coupled) as shown in Figure 5 for *Rps. acidophila* and *Rb. sphaeroides*. As discussed in ref 32, the B800 thermal broadening can be understood in terms of theory developed for isolated chromophores in solids. (Note that in Figure 5 there is no break near 150 K, establishing that the reversible (unpublished results) structural change near 150 K is subtle enough to affect only the strongly coupled BChl *a* molecules of the B850 ring.)

**Pressure-Dependent Studies of the B875 (LH1) Band.** The dependencies of the width and position of the B875 band at 98 K on pressure (*P*) are shown in Figure 6. Both vary linearly with pressure with rates of 0.12 and  $-0.60 \text{ cm}^{-1}/\text{MPa}$ . Linear broadening and shifting for  $Q_y \leftarrow S_0$  absorption bands has been reported for a number of photosynthetic complexes.<sup>56</sup> This is also the case for  $\pi\pi^*(S_1)$  states of isolated chromophores imbedded in polymers and proteins<sup>58–61</sup> for which, however, the shift rates are relatively small, about  $-0.05$  to  $-0.15 \text{ cm}^{-1}/\text{MPa}$ . Shift rates for photosynthetic complexes which are  $\geq 0.2 \text{ cm}^{-1}/\text{MPa}$  in magnitude signify strong pigment–pigment

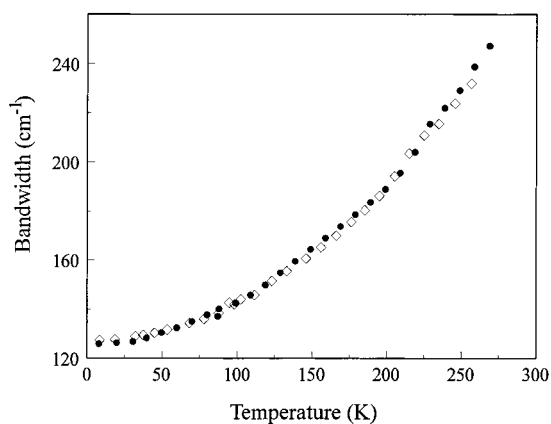


**Figure 5.** Thermal broadening of the B800 absorption band for LH2 of *Rb. sphaeroides* (diamonds) and *Rps. acidophila* (circles). Bandwidth values are full width at half-maximum.

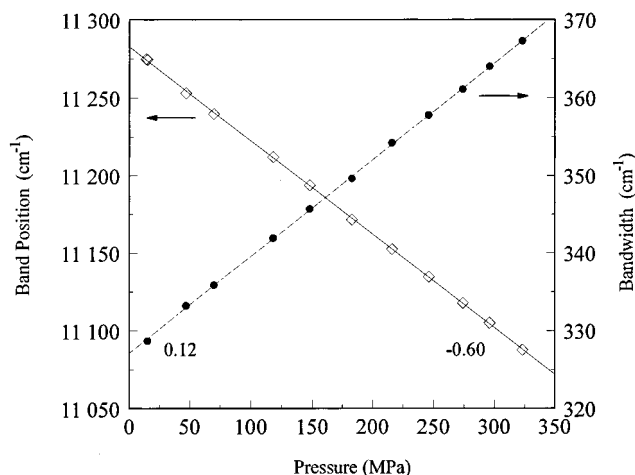


**Figure 6.** B875 band pressure shifting (diamonds) and broadening (circles) data for the LH1-only mutant of *Rb. sphaeroides* at 98 K. Linear shift (solid line) and linear broadening (dashed line) rates are  $-0.602 \pm 0.002 \text{ cm}^{-1} \text{MPa}^{-1}$  and  $0.120 \pm 0.003 \text{ cm}^{-1} \text{MPa}^{-1}$ , respectively.

interactions.<sup>8</sup> The effects of pressure ( $\leq 70 \text{ MPa}$ ) on the B875 band were determined at 12 K. The broadening rate was  $0.13 \pm 0.01 \text{ cm}^{-1}/\text{MPa}$  and the shift rate  $-0.63 \pm 0.02 \text{ cm}^{-1}/\text{MPa}$  (results not shown). That these rates are nearly the same as those at 98 K is consistent with the compressibility,  $\kappa$ , being weakly temperature dependent. These band shift rates are the largest yet observed for photosynthetic complexes.

In addition to determining the response of the absorption band to pressure, it is important to study the response of a single exciton level which contributes to the band. This is possible for B896 (also B870 of the B850 band<sup>32</sup>) since it is the lowest exciton level of the B875 ring and sharp ZPH can be burned into the inhomogeneously broadened B896 absorption profile, Figure 2. The linear pressure shifts for five holes burned into B896 with different burn frequencies at 12 K are shown in Figure 7. The ZPH spanned a range of about  $130 \text{ cm}^{-1}$ , from the high- to low-energy sides of the B896 absorption profile. The linear shift rates are about 10% greater than the  $-0.63 \text{ cm}^{-1}/\text{MPa}$  rate for the B875 band. There is some indication from the bottom four data sets that the shift rate increases on going from the blue to red sides of B896. This effect is more evident for B870 of *Rps. acidophila* and *Rb. sphaeroides*.<sup>32</sup> The average value of the pressure shift rate in Figure 7 is  $-0.67 \text{ cm}^{-1}/\text{MPa}$ . From Table 3, it is seen that the average shift rates for B870 of the above two species are 20% lower. Pressure results for the

**TABLE 3: Pressure-Dependent Data for Isolated LH2 from *Rps. acidophila* and *Rb. sphaeroides*, LH1-Only Mutant of *Rb. sphaeroides* at ~12 K, and FMO Complex from *Cb. tepidum* at 4.2 K**

| (cm <sup>-1</sup> MPa <sup>-1</sup> ) | <i>Rps. acidophila</i><br>LH2 <sup>a</sup> |       |       | <i>Rb. sphaeroides</i> |       |                  |       |       | <i>Cb. tepidum</i><br>FMO |
|---------------------------------------|--------------------------------------------|-------|-------|------------------------|-------|------------------|-------|-------|---------------------------|
|                                       | B800                                       | B850  | B870  | LH2 <sup>b</sup>       |       | LH1 <sup>d</sup> |       |       |                           |
|                                       |                                            |       |       | B800                   | B850  | B870             | B875  | B896  |                           |
| shift rate                            | -0.09                                      | -0.39 | -0.51 | -0.15                  | -0.38 | -0.54            | -0.63 | -0.67 | -0.10 <sup>c</sup>        |
| broadening rate                       | ~0                                         | 0.13  |       | ~0                     | 0.15  |                  | 0.13  | 0.07  |                           |

<sup>a</sup> Ref 32. <sup>b</sup> Ref 32. <sup>c</sup> Ref 49. <sup>d</sup> See the captions of Figures 5 and 6 for the uncertainty.

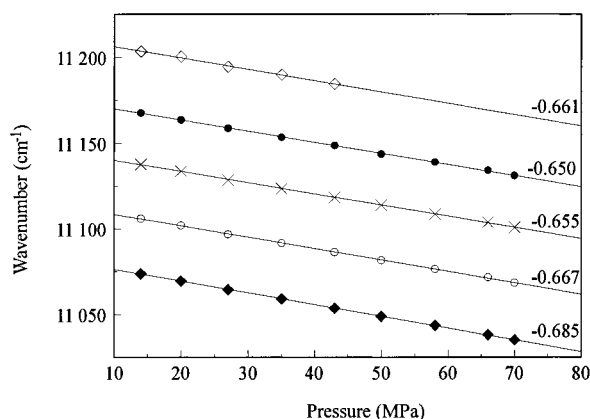


**Figure 7.** Linear pressure shifting of B896 ZPH (read resolution = 2 cm<sup>-1</sup>) for the LH1-only mutant of *Rb. sphaeroides*. Five holes were burned at 11 204, 11 201, 11 195, 11 190, and 11 185 cm<sup>-1</sup>, respectively, at 14 MPa and 12 K. A high burn fluence of 150 J/cm<sup>2</sup> was used, since holewidths were not the focus of this study. With increasing pressure, all holes shifted linearly (see the solid lines) to the red with rates (in cm<sup>-1</sup> MPa<sup>-1</sup>) given in the figure. Uncertainties = ±0.020, ±0.005, ±0.005, ±0.005, and ±0.003 cm<sup>-1</sup> MPa<sup>-1</sup> from top to bottom. For the pressure range used, no irreversible pressure shifting of B896 ZPH was observed (elastic behavior).

B800 band of LH2 from ref 32 are also given in Table 3 along with results for the BChl *a* antenna complex of *Cb. tepidum* from ref 49. Based on the discussions given in refs 8 and 49, the large pressure shifts for B850, B870, and B875 are indicative of strong excitonic coupling while, for example, the small shift for the B800 band is about that expected for an isolated chromophore.

Pressure broadenings of the B896 ZPH were determined, leading to an average broadening rate of 0.07 cm<sup>-1</sup>/MPa, about a factor of 2 lower than the rate for the B875 band.

#### 4. Discussion

The results presented above for the B875 band of the LH1 complex and the lowest energy B896 level compared with those for the B850 band and the lowest energy exciton level of the B850 ring (B870) indicate that the nearest BChl *a*–BChl *a* couplings of the B875 ring are at least as strong as those of the B850 ring. Given that the ZPH action spectra of B896<sup>62</sup> and B870 are similar (Figure 2) and that the LH1-only chromatophores show no absorption to higher energy of the B875 band (Figure 2) attributable to higher exciton levels of the LH1 BChl *a* molecules (*Q<sub>y</sub>* state), one can assume that the basic structural arrangement of these molecules around the ring is the same as that shown in Figure 1 for the B850 molecules. The LH1 structure of Hu et al.<sup>12</sup> determined by energy minimization and molecular dynamics calculations provides strong support. The absence of the just-mentioned absorptions indicates also that, for the LH1 complex, the energy disorder is not strong.<sup>35</sup> In this section we focus on the three questions posed at the end of the Introduction, the first of which has already been answered;

that is, the LH1 complex also undergoes a nonndenaturing structural change at ~150 K.

**Excitonic Level Structure in the Absence of Energy Disorder.** That the exciton levels of the B850 and B875 BChl *a* rings transform like the irreducible representations (reps) of a *C<sub>n</sub>* group is most apparent when one frames the problem in terms of a dimer of the ring. As noted in the Introduction, there are two choices for the dimer; see Figure 1. For either dimer the upper (u) level is essentially forbidden in absorption while the lower (l) is strongly allowed. Irrespective of the choice of dimer, the u- and l-levels spawn exciton manifolds for the *C<sub>n</sub>* ring. The projection operator technique of group theory<sup>63,64</sup> allows for generation of the exact eigenfunctions for both manifolds. In the nearest dimer–dimer coupling approximation which, of course, is less restrictive than the nearest monomer–monomer coupling approximation, the energies of the two exciton manifolds are given by<sup>33,43</sup>

$$E_l^j = e_l + 2V_l \cos(2\pi j/n) \quad (1)$$

and

$$E_u^j = e_u + 2V_u \cos(2\pi j/n) \quad (2)$$

where *e<sub>l</sub>* and *e<sub>u</sub>* are the energies of the two levels of the dimer, *V<sub>l</sub>* and *V<sub>u</sub>* are, respectively, the nearest neighbor dimer–dimer coupling energies for the lower and upper manifolds, and *j* = 0, 1, ..., *n* – 1 with *n* the number of dimers in the ring. For *n* = 9, the correspondence between *j* values and irreducible representations is *j* = 0(A); *j* = {1,8}(E<sub>1</sub>); *j* = {2,7}(E<sub>2</sub>); *j* = {3,6}(E<sub>3</sub>), and *j* = {4,5}(E<sub>4</sub>); see Figure 2. Following the generation of the u- and l-manifolds, one needs to consider the interactions between their respective exciton levels. The couplings are given by<sup>33,43</sup>

$$H_{ul}^j = 2V_{ul} \cos(2\pi j/n) \quad (3)$$

Because the Hamiltonian is totally symmetric, the coupling is restricted by symmetry to levels of the same *j* value. The dimer–dimer couplings *V<sub>l</sub>*, *V<sub>u</sub>*, and *V<sub>ul</sub>* can be determined using monomer–monomer coupling energies. The B850 exciton level structure shown in Figure 2 was calculated with *e<sub>u</sub>* – *e<sub>l</sub>* = 600 cm<sup>-1</sup>, *V<sub>u</sub>* = 100 cm<sup>-1</sup>, *V<sub>l</sub>* = –200 cm<sup>-1</sup>, and *V<sub>ul</sub>* = 130 cm<sup>-1</sup>, slightly rounded off values determined using the monomer–monomer coupling energies of Sauer et al.,<sup>5</sup> which were calculated using the room-temperature X-ray structure for LH2 of *Rps. acidophila*. As a result, the exciton level energy diagram in Figure 2 is quite similar to that of Sauer et al.<sup>5</sup>

It has been shown that<sup>32</sup> the A, E<sub>1</sub>, and E<sub>2</sub> levels associated with the B850 band (see Figure 2) are well described by eq 1, which we now write as

$$E_l^j = e_l + 2V_{dd} \cos(2\pi j/n) \quad (4)$$

where dd denotes dimer–dimer. (See Appendix for determi-

nation of  $V_{dd}$  from monomer–monomer coupling energies.) A value of  $-320\text{ cm}^{-1}$  for  $V_{dd}$  was used in ref 33 for the B850 band of *Rps. acidophila* in the low-temperature limit. This is larger than the  $-200\text{ cm}^{-1}$  value used to calculate the level diagram in Figure 2 since, according to ref 32, the value of  $V_{dd}$  for the low-temperature structure is about 35% larger than that for the high-temperature structure. In addition, utilization of the approximate Hamiltonian, eq 4, underestimates the level splittings by about 20% (results not shown). With  $V_{dd} = -320\text{ cm}^{-1}$  and  $n = 9$ , eq 4 results in a gap between the A (B870) and  $E_1$  levels ( $\Delta E$ ) of  $150\text{ cm}^{-1}$ . Inclusion of an acceptable level of static diagonal energy disorder increased  $\Delta E$  to the experimental value of  $200\text{ cm}^{-1}$  while yielding a percentage contribution from B870 to the total absorption intensity of the B850 band in reasonable agreement with the experimental value of 3–5%.<sup>33,34</sup> With  $n = 16$  and  $V_{dd} = -320\text{ cm}^{-1}$  for the B875 ring,  $\Delta E = 49\text{ cm}^{-1}$ , which is considerably smaller than the experimental values of 140 and  $120\text{ cm}^{-1}$  for the LH1-only mutant and *Rb. sphaeroides* chromatophores, Table 1. (If one uses the room-temperature value of  $V_{dd} = -200\text{ cm}^{-1}$ ,  $\Delta E = 30\text{ cm}^{-1}$ .) The large discrepancy between the experimental and calculated  $\Delta E$  values might suggest that  $V_{dd}$  for B875 is considerably larger than  $-320\text{ cm}^{-1}$ . However, whether this is the case cannot be determined without consideration of energy disorder. (As discussed in refs 9, 33, and 43 for the B850 ring of *Rps. acidophila*, static energy disorder (diagonal or off-diagonal) leads to an increase in  $\Delta E$  while, at the same time, bringing absorption intensity to the lowest energy exciton level (A symmetry) due to its mixing with the adjacent and strongly allowed  $E_1$  level, whose degeneracy is split by energy disorder.) We defer further consideration of this interesting problem until after the results of our pressure- and temperature-dependent studies are discussed.

**Pressure Effects on B875 and the B896 Exciton Level.** In earlier papers in which high pressure was combined with hole burning and absorption spectroscopies to study the excited electronic states of antenna and reaction center complexes, it was emphasized that linear pressure shifts greater than about  $-0.2\text{ cm}^{-1}/\text{MPa}$  are indicative of significant coupling between chlorophyll molecules.<sup>8</sup> By way of review, the linear pressure shifts (as measured by hole burning) for the  $S_1(\pi\pi^*) \leftarrow S_0$  transitions of isolated chromophores in polymers and glasses<sup>61</sup> and proteins<sup>59,60</sup> fall in the range  $-0.05$  to  $-0.15\text{ cm}^{-1}/\text{MPa}$ . In those works the equation

$$\Delta\nu/\Delta P = n\kappa 3^{-1}(\nu_m - \nu_{\text{vac}}) \quad (5)$$

was used to determine the value of the compressibility  $\kappa$ . The left-hand side is the pressure shift.  $n$  is the power of the attractive chromophore–solvent interaction ( $\propto R^{-n}$ ),  $\nu_m$  is the frequency of the hole at ambient pressure, and  $\nu_{\text{vac}}$  is the frequency of the optical transition in the gas phase. This equation emerges from the theory of Laird and Skinner<sup>65</sup> when the microscopic compressibility is replaced by the bulk compressibility  $\kappa$  of the host, which is assumed to be isotropic, homogeneous, and structurally random. When comparisons could be made, the values of  $\kappa$  obtained by hole burning (with  $n = 6$ ) were found to be in reasonable agreement with values determined by conventional methods. For the polymers, glasses, and proteins used,  $\kappa$  lies in the range  $0.05$ – $0.15\text{ GPa}^{-1}$ . When an absorption band is used to determine the pressure shift,  $\nu_m$  in eq 5 is the frequency of the absorption band maximum.

As discussed in refs 8 and 49, the Laird–Skinner theory is inapplicable to photosynthetic complexes characterized by strong excitonic coupling such as the special BChl pair of the reaction

center and the B850 and B875 rings of LH2 and LH1. (Unfortunately, a microscopic theory for the effects of pressure on excitonically coupled chromophores in proteins is not yet available.) However, when the chlorophyll pigments are well-separated, as is the case for the B800 molecules (Figure 1), the electrostatic interpigment couplings are weak and CT state effects are negligibly small. Thus, in ref 32 eq 5 was used with the low-temperature shift rate of the B800 band to estimate a value of  $\kappa$  for the LH2 complex. For the LH2 only NF 57 mutant and wild-type chromatophores of *Rb. sphaeroides*, the shift rates are close to  $-0.1\text{ cm}^{-1}/\text{MPa}$ . With  $\nu_{\text{vac}} = 13\,340\text{ cm}^{-1}$ ,<sup>66</sup> the value of  $\kappa$  is  $0.06\text{ GPa}^{-1}$ . In the present work the shift rate for B800 of the isolated LH2 complex of *Rps. acidophila* is  $-0.09\text{ cm}^{-1}/\text{MPa}$  (Table 3), which, with eq 5, yields a  $\kappa$  value close to  $0.05\text{ GPa}^{-1}$ . The shift rate for B800 of the isolated LH2 complex of *Rb. sphaeroides* is higher,  $-0.15\text{ cm}^{-1}/\text{MPa}$ , Table 3, which leads to  $\kappa \sim 0.09\text{ GPa}^{-1}$ . Another relevant example of a complex characterized by monomer-like pressure shifts is the Fenna–Matthews–Olson BChl *a* complex of *Cb. tepidum*. From the high-resolution X-ray structure of the FMO complex<sup>67</sup> it is clear that CT (electron-exchange) interactions are negligible. The pressure shifting of the ZPH of the lowest energy exciton level of the FMO complex yielded a value for  $\kappa$  of  $\sim 0.08\text{ GPa}^{-1}$ .<sup>49</sup>

Given the above results, we take  $0.1\text{ GPa}^{-1}$  as a reasonable typical value for the isotropic  $\kappa$  value of photosynthetic complexes in the low-temperature limit. (It is apparent from the results of refs 32 and 68 that the temperature dependence of  $\kappa$  is weak.) This is not to say that the compressibility tensors of complexes such as LH2 and LH1 are isotropic; their structures suggest otherwise.

With  $\kappa \sim 0.1\text{ GPa}^{-1}$ , we address the question of whether purely electrostatic BChl *a*–BChl *a* interactions can account for the large linear pressure shifts associated with the B850 and B875 BChl *a* rings of LH2 and LH1. From Table 3, the average shift for B870 of *Rps. acidophila* and *Rb. sphaeroides* is  $-0.51$  and  $-0.54\text{ cm}^{-1}/\text{MPa}$ , respectively, while the average shift for B896 of *Rb. sphaeroides* is  $-0.67\text{ cm}^{-1}/\text{MPa}$ . We use these shifts rather than those for the B850 and B875 absorption bands since these bands are contributed to by the two components of the allowed  $E_1$  level which are split apart by energy disorder; that is, the responses of the two components to pressure may be different. The calculations that follow assume, by necessity, that the protein matrix is homogeneous and isotropic. It will be seen that correction of the errors introduced by this assumption would be unlikely to alter our conclusion that electrostatic BChl *a*–BChl *a* interactions cannot account for the largeness of the above shifts.

In the point dipole–point dipole approximation<sup>69</sup> for electrostatic coupling between two BChl *a* chromophores, the fractional change in the coupling,  $V$ , for a pressure change  $\Delta P$  is given by<sup>49,70</sup>

$$\frac{\Delta V}{V} = \kappa \Delta P \quad (6)$$

where  $\Delta P$  is the pressure measured relative to ambient pressure ( $0.1\text{ MPa}$ ). The corresponding fractional change in  $R$ , the distance between the two point dipoles, is

$$\left| \frac{\Delta R}{R} \right| = 3^{-1} \kappa \Delta P \quad (7)$$

since  $V \propto R^{-3}$ . (For  $\Delta P = 0.35\text{ GPa}$  and  $\kappa = 0.1\text{ GPa}^{-1}$ ,  $|\Delta R/R| = 0.01$ .) For the B850 and B875 rings, we have argued

that eq 4 provides an adequate description for the  $E_1$  and  $A$  exciton levels, which contribute to the B850 and B875 absorption bands. For the B850 ring of *Rps. acidophila*, a value of  $V_{dd} = -320 \text{ cm}^{-1}$  was used for the low-temperature structure, vide supra. This value corresponds to a coupling of about  $+500 \text{ cm}^{-1}$  between the two nearest monomers of adjacent dimers (see the Appendix), which is  $\sim 200 \text{ cm}^{-1}$  larger than that calculated by Sauer et al.<sup>5</sup> for the room-temperature structure. As discussed, however, the nearest neighbor BChl  $a$ –BChl  $a$  couplings for the low-temperature structure are stronger by about 35%. Thus, we think that a value of  $+500 \text{ cm}^{-1}$  is reasonable. Given that the couplings at room temperature between the monomers which comprise the  $8.9 \text{ \AA}$  dimer and those which comprise the  $9.6 \text{ \AA}$  dimer (see Figure 1) are similar, we set the monomer–monomer coupling ( $V_{mm}$ ) of the “basic” dimer chosen for the development of the ring Hamiltonian (eqs 1–3) equal to  $500 \text{ cm}^{-1}$ . At this point we stack everything in favor of electrostatic interactions; that is, we consider that  $V_{dd} = -320 \text{ cm}^{-1}$  and  $V_{mm} = 500 \text{ cm}^{-1}$  are electrostatic so that an upper limit to the contribution from this type of interaction to the pressure shift can be determined. From the discussion that precedes eq 1 and eq 6, it follows that the pressure shift is

$$\frac{\partial \nu}{\partial P} \approx (2V_{dd} - V_{mm})\kappa \quad (8)$$

which, with the values for  $V_{dd}$ ,  $V_{mm}$ , and  $\kappa$  given above, leads to  $\partial \nu / \partial P = -0.11 \text{ cm}^{-1}/\text{MPa}$ . To this value should be added the shift rate expected from monomer–protein interactions, about  $-0.1 \text{ cm}^{-1}/\text{MPa}$  (vide supra), for a total shift rate of about  $-0.2 \text{ cm}^{-1}/\text{MPa}$ . The experimental shift rate for the B870 and B896 exciton levels is  $-0.52$  (average for *Rps. acidophila* and *Rb. sphaeroides*) and  $-0.67 \text{ cm}^{-1}/\text{MPa}$ , respectively. Thus, the discrepancy between experiment and the theoretical estimate is large.

For B896 and B870, the discrepancy is about  $-0.45$  and about  $-0.3 \text{ cm}^{-1}/\text{MPa}$ , respectively. By attributing the discrepancy to CT interactions, one can estimate a lower limit for the dependence of the CT coupling on an effective BChl  $a$ –BChl  $a$  distance ( $R_{CT}$ ) that controls this coupling. The X-ray structures of the LH2 complexes of *Rps. acidophila* and *Rs. molischianum* yield shortest interatomic distances between adjacent B850 BChl  $a$  molecules of  $\sim 3.5 \text{ \AA}$ .<sup>71</sup> The corresponding distances between tetrapyrrole planes are also about  $3.5 \text{ \AA}$ .<sup>71</sup> Thus, we set  $R_{CT}$  equal to  $3.5 \text{ \AA}$ . The interplanar separation between the overlapping pyrrole rings I of the special pair of the bacterial RC is  $3.3 \text{ \AA}$ . The electronic structure ( $Q_y$ ) calculations of Thompson and Fajer<sup>72</sup> on the special pair indicate that for small variations in this distance ( $< \pm 0.1 \text{ \AA}$ )

$$\frac{\Delta V_{CT}}{\Delta R_{CT}} \approx -A \quad (9)$$

where  $\Delta V_{CT}$  is the change in the CT coupling produced by a change in  $R_{CT}$  of  $\Delta R_{CT}$  and  $A$  is a constant. A value for  $A$  of  $\sim 270 \text{ cm}^{-1}/0.1 \text{ \AA}$  (at  $3.3 \text{ \AA}$ ) for the special pair was estimated<sup>8</sup> based on the results of Thompson and Fajer. In what follows we use eq 9 for the B850 and B875 rings. At this time,  $R_{CT}$  can only be said to be associated with an effective displacement coordinate important to CT. It follows with eqs 7–9 that

$$\left(\frac{\partial \nu}{\partial P}\right)_{CT} \approx -A\kappa R_{CT} \quad (10)$$

for the pressure shift when it is assumed that the CT coupling

between the monomers of the chosen dimer of the ring is equal to the CT coupling of nearest neighbors of adjacent dimers. (In eq 4,  $e_1$  is the energy of the lower energy level of the dimer. This level is responsible for one-third of the pressure shift in eq 10 with the remaining two-thirds coming from the  $2V_{dd} \cos(2\pi j/n)$  term in eq 4.) With  $\kappa = 0.1 \text{ GPa}^{-1}$ ,  $R_{CT} = 3.5 \text{ \AA}$ , and  $(\partial \nu / \partial P)_{CT} = -0.3 \text{ cm}^{-1}/\text{MPa}$  for the B850 ring, eq 10 yields  $A = 85 \text{ cm}^{-1}/0.1 \text{ \AA}$ . For B896,  $A = 126 \text{ cm}^{-1}/0.1 \text{ \AA}$ . The difference in the  $A$  values does not necessarily indicate that the BChl  $a$ –BChl  $a$  couplings of LH1 are stronger than those of the B850 ring since, for example, the  $\kappa$  and  $R_{CT}$  values for the two complexes may differ somewhat. That the values are smaller than the  $\sim 270 \text{ cm}^{-1}/0.1 \text{ \AA}$  value for the special pair is expected because of its shorter  $R_{CT}$  distance and shorter  $R_{Mg} \cdots Mg$  distance ( $7.2 \text{ \AA}$ ).

In summary, the large pressure shifting of the B850 and B875 absorption bands and their lowest energy exciton levels, B870 and B896, cannot be understood in terms of electrostatic interactions between BChl  $a$  molecules. Our model leads to the conclusion that charge-transfer (CT) states or, equivalently, electron-exchange interactions between neighboring BChl  $a$  molecules are mainly responsible for the largeness of the pressure shifts. Pressure-dependent data for  $Q_y$  absorption bands associated with BChl  $a$  molecules which are well-separated provide strong support for this conclusion. The value for  $A$  of  $\sim 100 \text{ cm}^{-1}/0.1 \text{ \AA}$  (average for B875 and B850) can serve as a benchmark for electronic structure calculations.

To conclude this subsection, we address the question of why the B800 bandwidth is independent of pressure while the widths of B850 and B875 increase significantly with increasing pressure, Table 3. We believe that the explanation is most likely linked to the fact that the B800 and B850/B875 BChl  $a$  molecules are weakly and strongly coupled, respectively. The results of our calculations on the effects of static, random diagonal energy disorder indicate that the states of the B800 ring are highly localized on individual molecules, while the exciton levels of the B850 ring still exhibit considerable delocalization.<sup>35</sup> Such a finding is consistent with the results of ref 9. The B850 and B875 absorption bands are contributed to mainly by the two components of the strongly allowed  $E_1$  level which are split apart by energy disorder. The results of ref 33 for the B850 ring (and unpublished results) show that the red shifting of the lower energy  $E_1$  component ( $E_{1,l}$ ) with increasing disorder is larger than that of the higher  $E_1$  component ( $E_{1,h}$ ). (The red shifting of B870 is even larger since it lies at the bottom of the exciton band.) Thus, if an increase in pressure increases the energy disorder, one has an explanation for the pressure broadening of the B850 and B875 bands. We note that the  $Q_y$  absorption band of the special pair of the *Rps. viridis* reaction center, P960, shows no pressure broadening<sup>8</sup> even though the coupling between the BChl molecules of the special pair is stronger than in the B850 and B875 rings. This is not inconsistent with our pressure broadening model since the upper dimer level of the special pair lies well to the blue ( $\sim 1900 \text{ cm}^{-1}$ ) of the P960 band. Finally, we note that the theory of Laird and Skinner<sup>65</sup> predicts an absence of broadening for an absorption band due to a localized transition when the inhomogeneous broadening stems from attractive intermolecular interactions between the chromophore and host. This may explain the absence of pressure broadening for B800.

**Temperature Dependence of the B875 Band of LH1.** We begin with the thermal broadening data for the B875 band shown in Figure 4 which show linear regions of broadening above and below  $150 \text{ K}$ , the temperature at which the structural change



occurs. The B850 bands of *Rps. acidophila*, *Rb. sphaeroides*, and *Rs. molischianum* exhibit the same behavior, the only difference being in the values of the linear broadening rates; see Table 2. For all these bands, the linear broadening for the low-temperature structure begins near 50 K. The thermal broadening of the B800 band of the LH2 complex is very different (Figure 5) and of the type consistent with a localized transition.<sup>32</sup> As pointed out in refs 31 and 32, linear broadening is consistent with downward relaxation between exciton levels by one-phonon emission.<sup>73</sup> This is because this non-Förster mechanism leads to the thermal factor  $(\bar{n}(\omega_{\text{pr}}) + 1)$  in the Fermi-Golden rule rate expression, where  $\bar{n}(\omega_{\text{pr}})$  is the thermal occupation number of the promoting mode with frequency  $\omega_{\text{pr}}$ . (For interexciton level relaxation the dynamics of the promoting mode must be such as to “wobble” the BChl *a* molecules, i.e., modulate BChl *a*–BChl *a* couplings.) The thermal occupation number is  $[\exp(\hbar\omega_{\text{pr}}/kT) - 1]^{-1}$ , which, in the high-temperature limit, equals  $(kT/\hbar\omega_{\text{pr}})$ . The Fermi-Golden rule expression for downward relaxation used in ref 32 is

$$k(T) = C \left( \frac{V^2}{\omega_{\text{pr}}\omega_{\text{ph}}} \right) (\bar{n}(\omega_{\text{pr}}) + 1) FC_{\text{ph}}(\Omega - \omega_{\text{pr}}) \quad (11)$$

where  $\Omega$  is the electronic energy gap and  $C$  is a constant which includes geometrical factors that define how the variation of  $V$  via the promoting mode is proportional to  $V$ .<sup>73</sup> When eq 4 is used for the A, E<sub>1</sub>, and E<sub>2</sub> levels associated with the B850 and B875 band,  $V = V_{\text{dd}}$  (see the Appendix). In ref 32, it was assumed that the downward relaxation is associated with the E<sub>1</sub> and A exciton levels. (Neglect of the E<sub>2</sub> levels is reasonable since it is weakly absorbing and does not contribute to the main part of the B850 absorption band.) However, energy disorder, diagonal and/or off-diagonal, splits the E<sub>1</sub> degeneracy,<sup>33,43</sup> meaning that one is confronted with a three-level system. Energy disorder further complicates the problem because it leads to a distribution of values for level spacings. In ref 33 it was argued that the average splitting of the E<sub>1</sub> level of the B850 band in the low-temperature limit ( $<150$  K) is  $\lesssim 60$  cm<sup>-1</sup>. Since nothing is known about the low-frequency vibrational/phononic dynamics of the LH2 and LH1 complexes, it is not possible to assess the relative contributions from the E<sub>1,h</sub>  $\rightarrow$  E<sub>1,l</sub>, E<sub>1,h</sub>  $\rightarrow$  A, and E<sub>1,l</sub>  $\rightarrow$  A relaxations to the thermal broadening. For this reason we will continue to consider that the broadening is due to relaxation between two exciton levels with an effective electronic energy gap of  $\Omega$ , cf. eq 11.

$FC(\Omega - \omega_{\text{pr}})$  in eq 11 is the frequency-dependent Franck–Condon factor for the low-frequency ( $\omega_{\text{ph}}$ ) protein (bath) modes involved in interexciton level relaxation. Its inclusion is required for energy conservation,  $\Omega = \omega_{\text{pr}} + \omega_{\text{ph}}$ , since it is unlikely that  $\omega_{\text{pr}}$  is equal to  $\Omega$ , especially when one takes into account energy disorder from structural heterogeneity. Such a FC factor should exist since the localization/extendedness patterns from energy disorder for the exciton levels differ significantly, even for weak energy disorder.<sup>35</sup> Since linear broadening begins near 50 K (a fairly high temperature given that the distributions of phonons that couple to the  $S_1(Q_y) \leftarrow S_0$  transitions have mean frequencies of about 20 cm<sup>-1</sup><sup>37,38</sup>), we consider the assumption made in ref 32 that the FC factor is weakly dependent on  $\omega_{\text{ph}}$  or, equivalently, that its temperature dependence is weak to be reasonable. This assumption is supported by the finding that the thermal broadenings ( $T \lesssim 150$  K) for the B850 bands of *Rps. acidophila*, *Rs. molischianum*, and *Rb. sphaeroides*<sup>31</sup> and the B875 band of *Rb. sphaeroides*, Figure 4, are well described by  $\bar{n}(\omega_{\text{pr}}) + 1$ . The solid curve below 150 K in Figure 4 is the fit obtained for B875 with its fwhm,  $\Gamma(T)$ , given by

$$\Gamma(T) = \Gamma_{\text{inh}} + \Gamma_{\text{h}}(\bar{n}_{\omega_{\text{pr}}} + 1) \quad (12)$$

with  $\Gamma_{\text{inh}}$ , the inhomogeneous broadening, set by the value of 150 cm<sup>-1</sup> for the inhomogeneous broadening of the B896 ZPH action spectrum, Figure 2. It is possible, however, that  $\Gamma_{\text{inh}}$  for the E<sub>1</sub> levels could differ somewhat from the value of 150 cm<sup>-1</sup> for P896. That  $\Gamma_{\text{inh}}$  can be taken to be temperature independent below  $\sim 150$  K is justified since the B875 band (also B850 bands) does *not* shift with temperature below 150 K; that is, anharmonic (thermal expansivity) effects are negligible.  $\Gamma_{\text{h}}$  is the homogeneous broadening due to interexciton relaxation in the limit as  $T \rightarrow 0$  K. In this limit,  $\Gamma = 250$  cm<sup>-1</sup> (Table 1), which is approximately equal to  $\Gamma_{\text{inh}} + \Gamma_{\text{h}}$ . Thus,  $\Gamma_{\text{h}} \approx 100$  cm<sup>-1</sup>. Finally, a value of 60 cm<sup>-1</sup> for  $\omega_{\text{pr}}$  was obtained from the fitting. The same procedure was used in ref 31 to obtain a value for  $\omega_{\text{pr}}$  of 70 cm<sup>-1</sup> for the B850 band of *Rps. acidophila*.

The question of whether the difference in the thermal broadening rates (slopes) for the B850 band of the low- and high-temperature structures of a given LH2 complex can be used to estimate the difference between the BChl *a*–BChl *a* coupling strengths for the low- and high-temperature structures has been addressed.<sup>32</sup> With the FC factor in eq 11 taken to be independent of temperature, it was shown that the difference in linear slopes for the high- and low-temperature structures is given by

$$\Delta s = \beta(C'V^2\omega_{\text{ph}}^{-1}) \quad (13)$$

where  $\beta$  is a constant defined by  $\Delta V = \beta V$  with  $V$  the value of  $V$  for the high-temperature structure and  $\Delta V$  the change due to the structural change at  $\sim 150$  K.<sup>74</sup> The constant  $C'$  contains  $C$  of eq 11 multiplied by  $\omega_{\text{pr}}^{-2}$  and a term from the FC factor. Under the just stated assumptions, the term in parentheses of eq 12 is the linear broadening rate for the high-temperature structure, which, for the B875 band, equals 0.84 cm<sup>-1</sup>/K, Figure 4. From Figure 4,  $\Delta s = -0.24$  cm<sup>-1</sup>/K, which leads to a value for  $\beta$  of  $-0.29$ , meaning that  $V$  for the low-temperature structure is about 30% larger than the value for the high-temperature structure. The percentage increase for the B850 bands of *Rps. acidophila* and *Rb. sphaeroides* is, respectively, 36 and 44%<sup>32</sup> (isolated LH2 complexes and chromatophores). That the thermal broadening and shifting of the B850 band for a given species are the same for the isolated LH2 complex and chromatophores<sup>32</sup> means that isolation is not responsible for the temperature effects and the structural change at 150 K.

The experimental results of Figure 4 for B875 and the analogous results for the B850 band of three species<sup>31,32</sup> establish that the LH1 and LH2 complexes undergo a structural change near 150 K. The temperature-dependent data for the B800 band, Figure 5, do not reveal the structural change. Furthermore, the position of the B800 band does not vary with temperature as the temperature is reduced from ambient to 4 K. Given that the B800 molecules are weakly coupled to each other, this means that the interactions between the B800 molecules and the protein matrix are “blind” to the structural change, which means that the changes in distances are too small to affect BChl *a*–protein residue and other nonexcitonic interactions. The structural change is probably too small to be seen by X-ray diffraction at a typical resolution of 2.5 Å. During the course of writing this paper, Prince et al. solved the LH2 structure to a resolution of 2.0 Å at 100 K (unpublished results). At this resolution, no significant structural difference is observed in comparison with the room-temperature structure obtained at 2.5 Å. The above discussion, plus the discussion in the preceding section on

pressure effects, lead us to conclude that the structural change at 150 K seen via the B850 and B875 absorption bands is due to a change in electron-exchange interactions between nearest neighbor BChl *a* molecules of the B850 and B875 rings or, equivalently, a change in the mixing of CT states with the  $Q_y$  states.<sup>9</sup> Equation 11 provides a basis for understanding the extent to which these interactions are stronger for the low-temperature structure.

To conclude this subsection we discuss the linear blue-shifting of the B875 band with temperature for the high-temperature structure,  $T > 150$  K, Figure 4. The shift rate is  $0.92 \text{ cm}^{-1}/\text{K}$ , which leads to a shift of  $\sim 140 \text{ cm}^{-1}$  as temperature is increased from 150 to 300 K. We note that the effects (physics) of increasing pressure at constant temperature are different from those of decreasing temperature at constant pressure as discussed by Sesselman et al. in their study of molecular chromophores imbedded in polymers.<sup>58</sup> For example, they show that the shift of the absorption frequency ( $\nu$ ) of a chromophore as the temperature is increased from  $T_1$  to  $T_2$  at constant pressure can be expressed as

$$\nu(T_2) - \nu(T_1) = \int_{T_1}^{T_2} \left( \frac{\partial \nu}{\partial T} \right)_P dT - 3 \left( \frac{\partial \nu}{\partial P} \right)_T \int_{T_1}^{T_2} \frac{\alpha_1}{\kappa} dT \quad (14)$$

where  $\alpha_1$  is the linear expansivity, the temperature dependence of which has been determined for polymers.<sup>76</sup> The first term on the rhs is generally negative, a consequence of a reduction in phonon frequencies upon electronic excitation of the chromophore. Since  $\alpha_1$  and  $\kappa$  are positive while  $(\partial \nu / \partial P)_T$  is negative, the second term is positive. Therefore, application of eq 14 to the B875 band's linear blue-shifting at temperatures above  $\sim 150$  K requires that the second term dominates the first. A simple calculation shows that this is reasonable. From our data we set  $(\partial \nu / \partial P)_T = -0.67 \text{ cm}^{-1}/\text{MPa}$  for B875. As mentioned, for polymers and proteins the temperature dependence of  $\kappa$  is weak. Since linear shift data at high temperatures are being considered, we set  $\kappa = 0.15 \text{ GPa}^{-1}$ . For polymers the temperature dependence of the expansivity is weak for  $T \gtrsim 150$  K. We use an average value of  $\alpha_1 = 6 \times 10^{-5} \text{ K}^{-1}$  for the temperature range 150–300 K based on the data of Lyon et al.<sup>77</sup> for poly-(methyl methacrylate), PMMA. With these values the second term of eq 14 yields a bandshift of  $120 \text{ cm}^{-1}$  for a temperature increase from 150 to 300 K, which is in reasonable agreement with the experimental values. Thus, one can be confident that the second term of eq 14 is largely responsible for the linear blue-shifting of the B875 band at temperatures above about 150 K. The above model has also been successfully applied to the blue-shifting of the B850 bands of *Rps. acidophila* and *Rb. sphaeroides*.<sup>32</sup> The absence of shifting at temperatures below 150 K can be understood, in part, by the strong nonlinear decrease in  $\alpha_1$  at lower temperatures. For example,  $\alpha_1$  (4 K) =  $2.7 \times 10^{-7} \text{ K}^{-1}$  and  $\alpha_1$  (50 K) =  $2.1 \times 10^{-5} \text{ K}^{-1}$  for PMMA. Also,  $\alpha_1$  may well undergo an additional decrease below 150 K due to the structural change. In addition, the first term in eq 14 is more likely to counterbalance the second term at lower temperatures.

Finally, the above model affords an explanation for why the B800 band of the LH2 complex does not shift with temperature above 150 K since its  $(\partial \nu / \partial P)_T$  value is a factor of about 7 times smaller than that of the B875 band.<sup>32</sup>

## 5. Conclusions and Final Remarks

Earlier studies on the effects of pressure on the  $Q_y(S_1 \leftarrow S_0)$  absorption bands and zero-phonon holes burned into them

established that pressure is a useful tool for identifying strong excitonic coupling between chlorophyll molecules in antenna and reaction center complexes. The key observables are the linear pressure shifts for the band and ZPH. Shift rates of magnitude  $\gtrsim 0.2 \text{ cm}^{-1}/\text{MPa}$  are indicative of strong coupling. The average shift rate reported here for the B896 (A) exciton level of the LH1 rings is  $-0.67 \text{ cm}^{-1}/\text{MPa}$ . The shift rate for the B875 band is 10% lower. The important question of whether electrostatic (e.g., transition dipole–transition dipole) interactions between BChl *a* molecules can account for these very large shift rates was addressed. A theoretical model was presented that indicates that the answer is no. We conclude that electron-exchange couplings between neighboring BChl *a* molecules of the LH1 (B875) ring are mainly responsible for the large pressure shifts. This conclusion also applies to the pressure shift rates for the B850 ring of the LH2 complex, which are about 20% lower than those of the B875 ring. The above conclusion means that a firm understanding of the excitonic structures of the B875 and B850 rings cannot be attained if electron-exchange interactions are neglected. Such interactions lead to CT states whose mixing with the  $Q_y(\pi\pi^*)$  states can have significant effects on excited-state electronic structure.<sup>9</sup>

Turning next to the results of temperature-dependent studies, the thermal broadening and shifting data for the B875 absorption band establish that, like the LH2 complex, the LH1 complex undergoes a structural change at  $\sim 150$  K, close to the glass transition temperature of the glycerol/water solvent. The structural change for LH2 is observed for chromatophores and isolated complexes. Thus, isolation is not responsible for the structural change. We predict that the structural change should occur in crystals, although the transition temperature may differ from 150 K. This reversible structural change is too small to be detected via the B800 absorption band associated with the weakly coupled B800 BChl *a* molecules. This, together with the results of the pressure experiments, indicates that detection of the structural change via the B850 and B875 bands is the result of changes in electron-exchange interactions between nearest neighbor BChl *a* molecules of the rings. As explained, very small changes in interatomic distances,  $\lesssim 0.1 \text{ \AA}$ , can strongly affect electron-exchange couplings. Thus, it seems unlikely that X-ray diffraction, at a resolution of  $\sim 2 \text{ \AA}$ , would be able to detect the structural change.

The dependences of the center frequency and width of the B875 absorption band on temperature are very similar to those reported earlier for the B850 band. The strong linear blue-shifting above 150 K was explained with the second term of eq 14, which one can approximate as  $-3(\partial \nu / \partial P)_T(\alpha_1/\kappa)(T_2 - T_1)$  since  $\alpha_1/\kappa$  carries a weak temperature dependence. The absence of shifting below 150 K is a consequence of the structural change and the strong, nonlinear decrease in  $\alpha_1$ . The absence of shifting for the B800 band is mainly due to its  $(\partial \nu / \partial P)_T$  value being a factor of about 7 times smaller than for B850 and B870, a consequence of weak excitonic coupling between B800 molecules.

As reported earlier for the B850 band, the thermal broadening of the B875 band above and below 150 K can be understood from eq 11, which governs the rate of downward interexciton level relaxation triggered by a promoting mode ( $\omega_{pr}$ ) with energy conservation ensured by participation of phonons ( $\omega_{ph}$ ). The linear broadening regions above and below 150 K, Figure 4, stem from the fact that  $\bar{n}(\omega_{pr}) + 1 \approx kT/\hbar\omega_p$  at sufficiently high temperatures. The nearest neighbor B875 BChl *a*–BChl *a* coupling(s) of the low-temperature structure are estimated to be 30% stronger than for the high-temperature structure.

**Acknowledgment.** Research at the Ames Laboratory was supported by the Division of Chemical Sciences, Office of Basic Energy Sciences, U.S. Department of Energy. Ames Laboratory is operated for USDOE by Iowa State University under Contract W-7405-Eng-82. Research at the University of Glasgow was supported by BBSRC and EU. We thank K. Schulten and X. Hu of the University of Illinois for providing us with structural information on the LH1 and LH2 complexes and W. W. Parson for discussions on CT interactions in the B850 ring of the LH2 complex. R.J.C. would like to thank Alexander von Humboldt Stiftung for the award of a research prize, Ms. Irene Geisenheimer for expert technical assistance, and Professor W. Lubitz for his hospitality in Berlin.

## Appendix

Following ref 5 we define  $A_1B_1$  and  $A_2B_2$  as nearest neighbor dimers where A and B designate the monomers of the dimer. The intermolecular potential energy that defines the interactions between monomers belonging to different dimers is

$$V = V_{B_1A_2} + V_{A_1A_2} + V_{A_1B_2} + V_{B_1B_2} \quad (\text{a1})$$

$V_u$ ,  $V_l$ , and  $V_{ul}$  of eq 1–3 are obtained from

$$\langle 2^{-1/2}(A_1^*B_1A_2B_2 \pm A_1B_1^*A_2B_2) | V | 2^{-1/2}(A_1B_1A_2^*B_2 \pm A_1B_1A_2B_2^*) \rangle \quad (\text{a2})$$

where the functions in the bra and ket are the normalized wave functions for dimer 1 and dimer 2, respectively. The ++, −, and +− combinations are  $V_u$ ,  $V_l$ , and  $V_{ul}$ , respectively. For example,

$$V_l \equiv V_{dd} = 2^{-1}(\langle V_{A_1A_2} \rangle + \langle V_{B_1B_2} \rangle - \langle V_{A_1B_2} \rangle - \langle V_{B_1A_2} \rangle) \quad (\text{a3})$$

with, for example

$$\langle V_{A_1A_2} \rangle = \langle A_1^*A_2 | V_{A_1A_2} | A_1A_2^* \rangle \quad (\text{a4})$$

The values for the four matrix elements in eq a3 from Sauer et al.<sup>5</sup> are, in order, −50, −36, 12, and 290  $\text{cm}^{-1}$ . (In the text  $\langle V_{B_1A_2} \rangle$ , the coupling between the nearest monomers, is referred to as  $V_{mm}$ .) They lead to  $V_u = 100 \text{ cm}^{-1}$ ,  $V_l \equiv V_{dd} = -200 \text{ cm}^{-1}$ , and  $V_{ul} = 130 \text{ cm}^{-1}$  (slightly rounded off values), which, with eqs 1–3, yielded the exciton energy level diagram for the B850 ring shown in Figure 2.

The bra and ket wave functions in eq a2 are not antisymmetrized; that is, electron-exchange is neglected. This neglect is justified for the  $A_1A_2$ ,  $B_1B_2$ , and  $A_1B_2$  monomer pairs but not the  $B_1A_2$  pair since  $B_1$  and  $A_2$  are nearest neighbors. We recall that the approximate Hamiltonian, eq 4, was used to describe the A,  $E_1$ , and  $E_2$  exciton levels of the B850 band of *Rps. acidiphila* and that, in the low-temperature limit,  $V_{dd} = -320 \text{ cm}^{-1}$ . The high-pressure data indicate that electron-exchange coupling between nearest neighbor BChl *a* molecules is very important. With  $V_{dd} = -320 \text{ cm}^{-1}$  it was estimated that  $V_{mm}$  is about +500  $\text{cm}^{-1}$ . The latter value was obtained by considering that only the  $\langle V_{B_1A_2} \rangle$  matrix element in eq a3 undergoes a significant increase below 150 K and using the room-temperature values for the other three matrix elements; the reasoning being that only  $\langle V_{B_1A_2} \rangle \equiv V_{mm}$  is contributed to by electron-exchange.

## References and Notes

- (1) van Grondelle, R.; Dekker, J. P.; Gillbro, T.; Sundström, V. *Biochim. Biophys. Acta* **1994**, *1187*, 1.

- (2) Pullerits, T.; Sundström, V. *Acc. Chem. Res.* **1996**, *29*, 381.
- (3) Sundström, V.; van Grondelle, R. In *Anoxygenic Photosynthetic Bacteria*; Blankenship, R. E., Madigan, M. T., Baller, C. E., Eds.; Kluwer Academic Publishers: Dordrecht, 1995; p 349.
- (4) Freer, A. A.; Prince, S. M.; Sauer, K.; Papiz, M. Z.; Hawthornthwaite-Lawless, A. M.; McDermott, G.; Cogdell, R. J.; Isaacs, N. W. *Structure* **1996**, *4*, 449.
- (5) Sauer, K.; Cogdell, R. J.; Prince, S. M.; Freer, A. A.; Isaacs, N. W.; Scheer, H. *Photochem. Photobiol.* **1996**, *64*, 564.
- (6) van der Laan, H.; Schmidt, Th.; Visschers, R. W.; Visscher, K. J.; van Grondelle, R.; Volker, S. *Chem. Phys. Lett.* **1990**, *170*, 231.
- (7) Reddy, N. R. S.; Cogdell, R. J.; Zhao, L. Small, G. J. *Photochem. Photobiol.* **1993**, *57*, 35.
- (8) Reddy, N. R. S.; Wu, H.-M.; Jankowiak, R.; Picorel, R.; Cogdell, R. J.; Small, G. J. *Photosyn. Res.* **1996**, *48*, 277.
- (9) Alden, R. G.; Johnson, E.; Nagarajan, V.; Parson, W. W.; Law, C. J. Cogdell, R. J. *J. Phys. Chem. B* **1997**, *101*, 4667.
- (10) Koepke, J.; Hu, X.; Muenke, C.; Schulten, K.; Michel, H. *Structure*, **1996**, *4*, 581.
- (11) Karrasch, S.; Bullough, P. A.; Ghosh, R. *EMBO J.* **1995**, *14*, 631.
- (12) Hu, X.; Ritz, T.; Damjanovic, A.; Schulten, K. *J. Phys. Chem. B* **1997**, *101*, 3854.
- (13) Papiz, M. Z.; Prince, S. M.; Hawthornthwaite-Lawless, A. M.; McDermott, G.; Freer, A. A.; Isaacs, N. W.; Cogdell, R. J. *Trends Plant Sci.* **1996**, *1*, 198.
- (14) Hess, S.; Chachisvilis, M.; Timpmann, K.; Jones, M.; Hunter, C. N.; Sundström, V. *Proc. Natl. Acad. Sci. U.S.A.* **1995**, *92*, 12333.
- (15) Jimenez, R.; Dikshit, S. N.; Bradforth, S. E.; Fleming, G. R. *J. Phys. Chem.* **1996**, *100*, 6825.
- (16) Wu, H.-M.; Savikhin, S.; Reddy, N. R. S.; Jankowiak, R.; Cogdell, R. J.; Struve, W. S.; Small, G. J. *J. Phys. Chem.* **1996**, *100*, 12022.
- (17) Savikhin, S.; Struve, W. S. *Chem. Phys.* **1996**, *210*, 91.
- (18) Nagarajan, V.; Parson, W. W. *Biochemistry* **1997**, *36*, 2300.
- (19) Chachisvilis, M.; Kühn, O.; Pullerits, T.; Sundström, V. *J. Phys. Chem. B* **1997**, *101*, 7275.
- (20) Nagarajan, V.; Alden, R. G.; Williams, J. C.; Parson, W. W. *Proc. Natl. Acad. Sci. U.S.A.* **1997**, *36*, 2300.
- (21) Kühn, O.; Sundström, V. *J. Phys. Chem. B* **1997**, *101*, 3432.
- (22) Reddy, N. R. S.; Small, G. J.; Seibert, M.; Picorel, R. *Chem. Phys. Lett.* **1991**, *181*, 391.
- (23) Fowler, G. J. S.; Hess, S.; Pullerits, T.; Sundström, V.; Hunter, C. N. *Biochemistry* **1997**, *36*, 11282.
- (24) Kolaczowski, S. V.; Hayes, J. M.; Small, G. J. *J. Phys. Chem.* **1994**, *98*, 13418.
- (25) De Caro, C.; Visschers, R. W.; van Grondelle, R.; Volker, S. *J. Phys. Chem.* **1994**, *98*, 10584.
- (26) Monshouwer, R.; de Zarate, I. O.; van Mourik, F.; van Grondelle, R. *Chem. Phys. Lett.* **1995**, *246*, 341.
- (27) Hess, S.; Åkesson, E.; Cogdell, R. J.; Pullerits, T.; Sundström, V. *Biophys. J.* **1995**, *69*, 2211.
- (28) Pullerits, T.; Chachisvilis, M.; Jones, M. R.; Hunter, C. N.; Sundström, V. *Chem. Phys. Lett.* **1994**, *224*, 355.
- (29) Bradforth, S. E.; Jimenez, R.; van Mourik, F.; van Grondelle, R.; Fleming, G. R. *J. Phys. Chem.* **1995**, *99*, 16179.
- (30) Reddy, N. R. S.; Picorel, R.; Small, G. J. *J. Phys. Chem.* **1992**, *96*, 6458.
- (31) Wu, H.-M.; Reddy, N. R. S.; Cogdell, R. J.; Muenke, C.; Michel, H.; Small, G. J. *Mol. Cryst. Liq. Cryst.* **1996**, *291*, 163.
- (32) Wu, H.-M.; Ratsep, M.; Jankowiak, R.; Cogdell, R. J.; Small, G. J. *J. Phys. Chem. B* **1997**, *101*, 7641.
- (33) Wu, H.-M.; Ratsep, M.; Lee, I.-J.; Cogdell, R. J.; Small, G. J. *J. Phys. Chem. B* **1997**, *101*, 7654.
- (34) Wu, H.-M.; Reddy, N. R. S.; Small, G. J. *J. Phys. Chem. B* **1997**, *101*, 651.
- (35) Wu, H.-M.; Small, G. J. *J. Phys. Chem. B* **1998**, *102*, 888.
- (36) van der Laan, H.; de Caro, C.; Schmidt, Th.; Visschers, R. W.; van Grondelle, R.; Fowler, G. J. S.; Hunter, C. N.; Volker, S. *Chem. Phys. Lett.* **1993**, *212*, 569.
- (37) Small, G. J. *Chem. Phys.* **1995**, *197*, 239.
- (38) Jankowiak, R.; Small, G. J. In *The Photosynthetic Reaction Center*, Vol. 2; Deisenhofer, J., Norris, J. R., Eds.; Academic Press: New York, 1993; p 133.
- (39) Jankowiak, R.; Hayes, J. M.; Small, G. J. *Chem. Rev.* **1993**, *93*, 1471.
- (40) Visschers, R. W.; van Mourik, F.; Monshouwer, R.; van Grondelle, R. *Biochim. Biophys. Acta* **1993**, *1141*, 238.
- (41) Pullerits, T.; van Mourik, F.; Monshouwer, R.; Visschers, R. W.; van Grondelle, R. *J. Lumin.* **1994**, *58*, 168.
- (42) Monshouwer, R.; Abrahamsson, M.; van Mourik, F.; van Grondelle, R. *J. Phys. Chem. B* **1997**, *101*, 7241.
- (43) Wu, H.-M.; Small, G. J. *Chem. Phys.* **1997**, *218*, 225.
- (44) Meier, T.; Zhao, Y.; Chernyak, V.; Mukamel, S. *J. Chem. Phys.* **1997**, *107*, 3876.

- (45) Leupold, D.; Stiel, H.; Teuchner, K.; Nowak, F.; Sandner, W.; Ücker, B.; Scheer, H. *Phys. Rev. Lett.* **1996**, *77*, 4675.
- (46) Meier, T.; Chernyak, V.; Mukamel, S. *J. Phys. Chem. B* **1997**, *101*, 7332.
- (47) Cogdell, R. J.; Hawthornthwaite, A. M. In *The Photosynthetic Reaction Center*; Deisenhofer, J., Norris, J. R., Eds.; Academic Press: San Diego, 1993; Vol. 1, p 23.
- (48) Lyle, P. A.; Kolaczowski, S. V.; Small, G. J. *J. Phys. Chem.* **1993**, *97*, 6926.
- (49) Reddy, N. R. S.; Jankowiak, R.; Small, G. J. *J. Phys. Chem.* **1995**, *99*, 16168.
- (50) Noguti, T.; Go, N. *Proteins* **1989**, *5*, 97.
- (51) Frauenfelder, H.; Alberding, N. A.; Ansari, A.; Braunstein, D.; Cowen, B. R.; Hong, M. K.; Iben, I. E. T.; Johnson, J. B.; Luck, S.; Marden, M. C.; Mourant, J. R.; Ormos, P.; Scholl, R.; Schulte, A.; Shyamsunder, E.; Sorensen, L. B.; Steinbach, P. J.; Xie, A.; Young, R. D.; Yue, k. T. *J. Phys. Chem.* **1990**, *94*, 1024.
- (52) The B850 BChl *a*–BChl *a* coupling energies of Sauer et al.<sup>5</sup> based on the room-temperature X-ray coordinates were used to calculate dimer–dimer coupling energies; see the Appendix.
- (53) In ZPH spectroscopy one burns a series of persistent ZPH across the inhomogeneously broadened absorption profile at constant burn fluence; see refs 32 and 34 for details.
- (54) Ansari, A.; Berendzen, J.; Braunstein, D.; Cowen, B. R.; Frauenfelder, H.; Hong, M. K.; Iben, I. E. T.; Johnson, J. B.; Ormos, P.; Sauke, T. B.; Scholl, R.; Schulte, A.; Steinbach, P. J.; Vittitow, J.; Young, R. D. *Biophys. Chem.* **1987**, *26*, 337.
- (55) Iben, I. E. T.; Braunstein, D.; Doster, W.; Frauenfelder, H.; Hong, M. K.; Johnson, J. B.; Luck, S.; Ormos, P.; Schulte, A.; Steinbach, P. J.; Xie, A. H.; Young, R. D. *Phys. Rev. Lett.* **1989**, *62*, 1916.
- (56) Pressures used were  $\leq 700$  MPa. Apparently, much higher pressures are required to observe nonlinear behavior (see, for example, ref 57).
- (57) Berg, O.; Chronister, E. L. *J. Chem. Phys.* **1997**, *106*, 4401.
- (58) Sesselmann, Th.; Richter, W.; Haarer, D.; Morawitz, H. *Phys. Rev. B* **1987**, *36*, 7601.
- (59) Zollfrank, J.; Friedrich, J.; Fidy, J.; Vanderkooi, J. M. *J. Chem. Phys.* **1991**, *94*, 8600.
- (60) Zollfrank, J.; Friedrich, J.; Parak, F. *Biophys. J.* **1992**, *61*, 716.
- (61) Zollfrank, J.; Friedrich, J. *J. Phys. Chem.* **1992**, *96*, 7889.
- (62) Determined earlier for chromatophores of *Rb. sphaeroides*: Reddy, et al. *J. Phys. Chem.* **1992**, *96*, 6458. In this reference, the inhomogeneous width of B896 was stated in the text as  $\sim 70$   $\text{cm}^{-1}$ . This is incorrect, as is obvious from Figure 3 of that paper. The correct value is  $\sim 140$   $\text{cm}^{-1}$ , close to the value reported here, Table 1.
- (63) Tinkham, M. *Group Theory and Quantum Mechanics*; McGraw-Hill: New York, 1964.
- (64) Hochstrasser, R. M. *Molecular Aspects of Symmetry*; W. A. Benjamin Inc.: New York, 1966.
- (65) Laird, B. B.; Skinner, J. L. *J. Chem. Phys.* **1989**, *90*, 3274.
- (66) Renge, I. *Chem. Phys.* **1992**, *167*, 173.
- (67) Matthews, B. W.; Fenna, R. E. *Acc. Chem. Res.* **1980**, *13*, 309.
- (68) Perepechko, I., Ed. *Low-Temperature Properties of Polymers*; Pergamon: Oxford, 1980.
- (69) According to Sauer et al.<sup>5</sup> use of the more accurate point-monopole approximation leads to a slight reduction of BChl *a*–BChl *a* nearest neighbor interaction energies for the B850 ring.
- (70) Gafert, J.; Friedrich, J.; Parak, F. *J. Chem. Phys.* **1993**, *99*, 2478.
- (71) Hu, X.; Schulten, K. Private communication.
- (72) Thompson, M. A.; Fajer, J. *J. Phys. Chem.* **1992**, *96*, 2933.
- (73) Davydov, A. S. *Theory of Molecular Excitons*; Plenum Press: New York, 1971.
- (74) It was assumed that  $\omega_{\text{pr}}$  changes little upon the structural change. Since  $\Omega = \omega_{\text{pr}} + \omega_{\text{ph}}$  and  $\Delta\Omega \approx \Delta V$ ,  $\Delta\omega_{\text{ph}} = \beta\omega_{\text{ph}}$ ; see ref 32 for details.
- (75) We predict that the same effects would be observed for crystals of the isolated LH2 complex, although the temperature at which the structural change occurs may differ from 150 K.
- (76) Lyon, K. G.; Salinger, G. L.; Swenson, C. A. *Phys. Rev. B* **1979**, *19*, 4231.